Accurate Kinetic Modeling of Alkaline Phosphatase in the *Escherichia coli* Periplasm: Implications for Enzyme Properties and Substrate Diffusion†

Michael B. Martinez, Michael C. Flickinger, and Gary L. Nelsestuen*

Department of Biochemistry, University of Minnesota, St. Paul, Minnesota 55108

Received August 18, 1995; Revised Manuscript Received November 16, 1995⊗

ABSTRACT: Alkaline phosphatase in the periplasm of *Escherichia coli* presents many of the complex factors that may influence enzymes *in vivo*. These include an environment that contains a high enzyme concentration, is densely populated with other macromolecules, and is separated from other compartments by a partial diffusion barrier. A previous study provided a partial description of this situation and developed a model that utilized kinetic behavior to estimate the permeability of the outer membrane [Martinez, M. B., et al., (1992) *Biochemistry 31*, 11500]. This study extends that description to provide a complete model for the enzyme at all substrate levels. Some of the parameters needed for complete modeling include the following: outer membrane permeability to the substrate and product, catalytic efficiency of the enzyme, number of enzymes per cell, and effects of the reaction product (an inhibitor) on the enzyme. The theoretical model fit the data quite well over a wide range of values for each of these parameters. The best fit of theory with experimental data required that the rate constant for product escape from the periplasm was 4-fold greater than that for substrate entry. This correlated with the relative sizes of the substrate and product. The excellent fit of theory and results suggested that alkaline phosphatase and its substrate were unaffected by the solution conditions in the periplasm. That is, the catalytic parameters (k_{cat} and K_M), determined for the enzyme in dilute solution, appeared to be unchanged by the conditions in the periplasm. The major factor that altered the kinetic behavior was the combined effect of the permeability barrier and the dense population of enzyme molecules in the periplasm. Given the large impact of these parameters on reaction properties, the excellent fit of theory and results was striking. Overall, this study demonstrated that enzyme action in the complex biological environment can be accurately modeled, if all factors that influence enzyme behavior are known.

Enzyme kinetic studies are usually conducted under steady state conditions where dilute enzyme and excess substrate are free to diffuse as individual particles. While one goal of such studies is to provide an estimate of enzyme behavior *in vivo*, the latter may provide conditions that differ from those of *in vitro* kinetic studies. Examples include the facts that biological situations often contain high enzyme concentrations, they may contain barriers to diffusion, and there may be limited diffusional space due to crowding by other macromolecules. The latter may influence the enzyme-catalyzed reaction by simple volume displacement or by direct interaction with the enzyme (Zimmerman, 1993). For example, solution crowding by 5% poly(ethylene glycol) caused a decrease in the K_M of hyaluronate lyase from 38.5 to 28.0 μg/mL (Laurent, 1971). Poly(ethylene glycol) lowered the K_M of lactic dehydrogenase for all of its substrates by about 50%. The solution conditions in biological systems may be modified more extensively than in these model systems. Solution crowding has also been suggested to have an effect on the thermodynamic properties of proteins (Laurent, 1963a,b, 1971; Minton, 1983).

Altered behavior of over-expressed enzymes or receptors (Abbott & Nelsestuen, 1987, 1988; Goldstein & Wiegel, 1983; Goldstein, 1989; Wiley, 1988) is another concern. For example, enzymes may normally associate with specific sites in the cell, so that overproduction may produce altered environments and/or inclusion bodies (Georgiou et al., 1986). Kinetic models have been developed to describe a similar situation where enzymes are immobilized on solid supports (Goldstein, 1976; Laidler & Bunting, 1980; Sundaram et al., 1970) and a facilitated diffusion enzyme reaction (ter Kuile & Cook, 1994). While many of these factors will vary with individual enzymes, some effects will be universal. One universal outcome of high enzyme density can be the attainment of the "perfectly reactive state". This condition exists when virtually every substrate molecule that diffuses to the vicinity of the enzyme population is converted to product (Martinez et al., 1992).

Unfortunately, high enzyme concentrations and limited ability to introduce substrate to these enzymes can limit the number of opportunities to examine *in vivo* enzyme kinetic parameters. One accessible condition where all of these complicating factors are present is the periplasm of Gram-negative bacteria, such as *Escherichia coli*. In this system, the perfectly reactive state was reached when the substrate concentration in the medium was low (Martinez et al., 1992), so that enzyme velocity was dependent on the number of collisions between cell and substrate and the permeability of the cell's outer membrane. At high substrate concentrations, the reaction reverted to conditions appropriate for analysis by the steady state Michaelis−Menten model.

† Supported in part by Grant HL15728 from the National Institutes of Health. M.B.M. was supported by an administrative supplement to grant HL15728 for support of members of ethnic groups who are underrepresented in the biomedical sciences. He was also the recipient of a grant from the Merck Chemical Co.

* Corresponding author: Gary L. Nelsestuen, Department of Biochemistry, 1479 Gortner Ave., St. Paul, MN 55108; telephone (612) 624-3622; fax (612) 625-5780; e-mail, gary-N@molbio.cbs.umn.edu.

⊗ Abstract published in *Advance ACS Abstracts,* January 15, 1996.

0006-2960/96/0435-1179$12.00/0

The restricted diffusion provided by the outer membrane enhanced the ability to reach the perfectly reactive state. Strains with more restrictive outer membranes require fewer enzymes or lower k_{cat}/K_M ratios than cells with a less restrictive outer membrane. The outer membrane permeability could be described by the term $f(a)$, the portion of collisions between the cell and substrate that resulted in the entry of substrate into the periplasm (Martinez et al., 1992).

This study presents a more comprehensive analysis of the kinetics of alkaline phosphatase in the *E. coli* periplasm. With the reasonable assumption that the rate constant for product (phosphate) escape from the periplasm was 4-fold greater than that for substrate (*p*-nitrophenyl phosphate) entry, this model fit the kinetic results for a wide range of cell properties, including normal and over-expressed enzyme levels. This suggested that the enzyme kinetic parameters determined in dilute solution were applicable to this enzyme *in vivo*. No correction for altered behavior due to solution crowding or other factors appeared to be necessary.

MATERIALS AND METHODS

Media and Reagents. *p*-Nitrophenyl phosphate (*p*-npp),[1] isopropyl β-D-thiogalactoside, *o*-carboxyphenyl phosphate (*o*-cpp), and other chemicals were purchased from the Sigma Chemical Company. Tryptone broth contained 10 g of bactopeptone (Difco Laboratories) and 5 g of NaCl per liter (Adler, 1973).

Cell Growth. All media contained ampicillin (100 μg/mL). Cells were inoculated into Tryptone broth from a freezer culture and were grown overnight at 30 °C in an Orbital shaker at 300 rpm. These cells were used to inoculate new media, and subsequent growth was at 37 °C unless indicated. Alkaline phosphatase was induced in plasmid-containing strains (see the following) by the addition of isopropyl β-D-thiogalactoside (IPTG, 1 mM) to the growth medium. There was a linear relationship between enzyme activity per cell and induction time (data not shown).

Cells were harvested in logarithmic growth and at a density of less than 6×10^8 cells/mL. Cell density was estimated by optical density at 590 nm, where a value of 1.0 (path length = 1 cm) corresponds to 6×10^8 cells/mL (Adler, 1973). In most cases, the harvested cells were placed on ice and stored overnight for use the next day. Storage for this period of time did not appear to influence the results. Cells were centrifuged for 10 min at 3000*g* and resuspended in the buffer used for enzyme assay. The methods of growth and induction of alkaline phosphatase in wild-type cells have been described previously (Martinez et al., 1992).

E. coli Strains. Strains K12 (wild type), MZ9387 pIV26, M703CE, and M464E have been described previously (Martinez et al., 1992; Schendel et al., 1989). All strains except K12 contained the pIV26 plasmid, which has the *phoA* gene linked to the lac promoter. Strains K12pIV26 and M701FE were generated by transformation of the parent strains, K12 (wild type) and JF701 (strain no. 6045, E. coli Genetic Stock Center, Yale University; *proC24, aroA357, his-53, ompC264, purE41, ilv-277, met-65, lacY29, xly-14, rpsL97, cycA1, cycB2?, tsx-63,* λ^-), with the pIV26 plasmid as described previously for the other strains (Martinez et al., 1992). Strain JF701 was further modified to contain a *phoA* deletion and an F′ plasmid, which has the *lacIq* gene, as previously described for the other strains (Martinez et al., 1992). The TEM type 1 β-lactamase gene was also present (Schendel et al., 1989; Sutcliffe, 1978). The different strains and porin expression under the growth conditions used include the following: K12 and K12pIV26 express both OmpF and OmpC in a wild-type manner. MZ9387 pIV26 expresses OmpC and OmpF in a wild-type manner and PhoE in a constitutive manner. M464E expresses PhoE constitutively, but does not express OmpC or OmpF. M703CE expresses only OmpC under the growth conditions used. Strain M701FE expresses only OmpF under the growth conditions used.

Enzyme Assays. All components of the enzyme assay were warmed to the 37 °C. The assay was initiated by the addition of cells. The assay volume was 1.0 mL. Absorbance measurements were obtained with a Beckman DU 70 spectrophotometer equipped with a water-jacketed cuvette holder. Readings were taken every 20 s for a total of 2 min. The average of these six measurements minus background (see the following) was used to calculate enzyme reaction velocity. The experimental range for these six readings was very low, normally less than ±2%. Replicate readings gave similar low standard deviations and are presented in a representative manner in the experiments presented here.

Maximum velocity was measured after cell lysis as described previously (Martinez et al., 1992). The substrate concentration (3.8 mM) was adequate to saturate the free enzyme ($K_M = 0.015$ mM). Standard deviations for at least three readings were less than ±3% of the values reported.

The substrate was *p*-nitrophenyl phosphate (*p*-npp), and the concentration of the product, *p*-nitrophenol, was monitored at 410 nm (extinction coefficient in assay buffer = 7800 M^{-1} cm^{-1}; Martinez et al., 1992) . The assay buffer was 0.1 M MOPS (pH 7.2) containing 86.0 mM NaCl and 1.0 mM $MgCl_2$.

Enzyme activity that had been released from the periplasm was measured and subtracted as background. Briefly, cells were incubated at the assay temperature for the time of the enzyme assay. They were centrifuged at 13000*g* for 3 min at room temperature. Alkaline phosphatase activity in the supernatant was determined with 3.8 mM substrate. This activity was subtracted from the experimental readings as background. Enzyme released from the cells was always less than 5% of the total activity present.

Inhibition Assays. Two compounds were used for inhibition experiments: inorganic phosphate, a competitive inhibitor, and *o*-carboxyphenyl phosphate (*o*-cpp), an alternative substrate. The latter is hydrolyzed by alkaline phosphatase to yield inorganic phosphate and *o*-carboxyphenol. At pH 7.2, *o*-cpp undergoes some spontaneous hydrolysis, so that inhibition was due to both *o*-cpp and inorganic phosphate. Hydrolysis of *o*-cpp can be monitored at 300 nm, but showed no absorbance at 410 nm, the wavelength used to monitor the hydrolysis of *p*-npp.

Theoretical Modeling. An earlier study showed that the kinetic behavior of enzymes sequestered in the *E. coli* periplasm conformed to the expectations for a diffusion-limited reaction. A modified form of the relationship developed by Berg and Purcell for receptor−ligand association (Berg & Purcell, 1977; Martinez et al., 1992) was used to describe the reaction. Berg and Purcell showed that the

[1] Abbreviations: *p*-npp, *p*-nitrophenyl phosphate; *o*-cpp, *o*-carboxyphenylphosphate.

observed rate constant for a binding interaction is the product of two terms: the rate constant for particle collision in solution (k_{coll}) and the probability that binding to a receptor will occur after collision:

$$k_{obs} = \left(\frac{4\pi N_A Da}{1000}\right)\left(\frac{Ns}{Ns + \pi a}\right) = k_{coll}\left(\frac{Ns}{Ns + \pi a}\right) \quad (1)$$

N_A is Avogadro's number, a is the sum of the radii of the colliding particles (a spherical shape was assumed and a effectively becomes equal to the radius of the larger particle), D is the sum of their diffusion constants (effectively that of the smaller particle), s is the effective capture radius of the receptor binding site, and N is the number of vacant receptors/cell.

For an enzyme in the periplasm of *E. coli*, eq 1 must be modified by a term, $f(a)$, which is the portion of ligand−cell collisions that result in the entry of substrate into the periplasm. This is a constant for each cell but varies with cell type, depending on the permeability of the outer membrane. For an enzyme, s is further modified by $f(s)$, which describes the portion of binding events that result in product formation. Thus, eq 2 is the general description of the rate constant for product formation by an enzyme in the *E. coli* periplasm, and eq 3 is the general equation for enzyme velocity.

$$k_{obs}' = \left(\frac{4\pi N_A D}{1000}\right) a(f(a))\left(\frac{Ns(f(s))}{Ns(f(s)) + \pi a f(a)}\right) \quad (2)$$

$$v = k_{obs}'[\text{cell}][\text{S}] \quad (3)$$

The previous study showed that two extreme types of kinetic behavior could be observed. The first occurred at low substrate concentrations where the number of unoccupied enzymes was large, so that $Nsf(s) \gg \pi af(a)$. The probability of product formation from substrate entering the periplasm approached 1.0, and the reaction velocity was described by

$$v = \left(\frac{4\pi N_A Da}{1000}\right) f(a)[\text{S}][\text{cell}] \quad (4)$$

Under these conditions, velocity was proportional to substrate concentration, and Eadie−Hofstee plots gave a slope of 0 (Martinez et al., 1992).

The other extreme occurred at high substrate concentrations where the number of unoccupied enzymes was low, so that $\pi af(a) \gg Nsf(s)$, and the reaction velocity was described by eq 5, the equivalent of the Michaelis−Menten relationship:

$$v = \left(\frac{4N_A Ds}{1000}\right) f(s)[\text{E}][\text{S}] \quad (5)$$

The earlier studies did not attempt to describe $f(s)$ in the cell or to determine whether the entire spectrum of enzyme velocity could be described by these relationships. The following allows the complete solution of this relationship.

Terms in eq 3 were consolidated to produce eq 3′:

$$v = \frac{A(N_{tot}(1 - v/V_{max}))B}{(N_{tot}(1 - v/V_{max}))B + \pi a f(a)} \quad (3')$$

Equation 3′ was rearranged and solved as a quadratic:

$$v^2 BN_{tot}/V_{max} - v(BN_{tot} + \pi a f(a) + AB[\text{cell}][\text{S}]N_{tot}/V_{max}) + ABN_{tot}[\text{cell}][\text{S}] = 0 \quad (6)$$

Identity of Terms in eq 3′. $N_{tot}(1 - v/V_{max})$ is the number of free enzyme sites per cell and is the appropriate value to use in eq 3. N_{tot} per cell was calculated from V_{max} for the cells used in the assay, the number of cells per assay, and k_{cat} for the enzyme.

A in eq 6 is the rate constant for substrate entry into the periplasm ($4\pi N_A Daf(a)/1000$), where D is the diffusion constant of the substrate (7.5×10^{-6} cm^2/s at 37 °C), a is the radius of the cell (0.5 μm was used for all calculations), and $f(a)$ is the portion of substrate−cell collisions that result in entry into the periplasm. As described in detail previously (Martinez et al., 1992), $f(a)$ was equal to the rate constant for product formation expressed on the basis of cell concentration and obtained under reaction conditions described by eq 4 (velocity limited by substrate entry into the periplasm), divided by the rate constant for the collision of substrate and cell ($k_{coll} = 2.8 \times 10^{12}$ M^{-1} s^{-1} at 37 °C).

B is the effective capture radius of a single enzyme ($s(f(s))$ and was obtained from eq 1, using $k_{obs} = k_{cat}/K_M$ (values for the free enzyme). Thus, in the absence of any inhibitor, $B = (k_{cat}/K_M)1000/4N_A D$. However, B is further complicated by the presence of a competitive inhibitor such as phosphate. In this case, $K_{M(app)}$ must be used in eq 1 and $B = (k_{cat}/K_M(1 + [\text{I}]/K_I))1000/4N_A D$. If inhibitor is added to the solution ($[\text{I}]_{added}$), diffusional equilibrium with the periplasm will be reached quickly, so that the concentration of inhibitor from this source should equal the concentration added to the assay buffer.

A more complex problem is presented by the product of the reaction, phosphate, which is an inhibitor whose concentration in the periplasm, $[\text{I}]_{in}$, will vary with the velocity of the reaction and the rate of escape of product from the periplasm. The impact of this source of inhibitor was estimated in the following manner: The rate constant for product escape from the periplasm was first assumed to be equal to that for substrate entry. In this case, $[\text{I}]_{in}$ will equal $[\text{S}]_{out}$ under conditions where all substrate molecules that enter the periplasm are converted to product (effectively, $[\text{S}]_{in} = 0$). The value of $v/[\text{S}]_{out}$ under this condition (v is proportional to [S]; Eadie−Hofstee plots are horizontal) was measured experimentally and is represented by the term Y. The value of $[\text{I}]_{in}$ was then obtained from the relationship, $[\text{I}]_{in} = v/Y$, for any experimental value of v.

Since the product is smaller than the substrate, its larger diffusion coefficient and easier passage through the porins should result in a larger rate constant for escape than for substrate entry. Another term, x, the ratio of the rate constant for product escape divided by that for substrate entry, was added to accommodate this difference. In this case, $[\text{I}]_{in} = v/xY$. The value of x should be larger than 1.0 and can be adjusted to create an optimum fit of the data. Finally, if an external inhibitor is also added, the total concentration of inhibitor inside the periplasm becomes the sum of both sources:

$$[\text{I}]_{tot} = v/xY + [\text{I}]_{added} \quad (7)$$

Theoretical curves for reaction velocity were obtained from eq 6 by solving for v at 22 different substrate concentrations, assuming no inhibition by reaction product in the periplasm.

The resulting velocities were then used to estimate $[I]_{in}$, from which new $K_{M(app)}$ values were obtained. These were then used to solve eq 6 to obtain a second set of values for velocity. This process was repeated until a constant value of v was obtained in subsequent calculations (two cycles were sufficient to eliminate significant changes). Smooth curves drawn through this series of points created the theoretical curves.

RESULTS

Theoretical Behavior. The kinetic behaviors of enzymes in the periplasm are highly influenced by the relative values of $Nsf(s)$ and $\pi af(a)$ (eq 2). Figure 1A shows the effect of variations in $sf(s)$ created by changing K_M via the addition of a competitive inhibitor. The latter increased $K_{M(app)}$ and altered curve shape without altering V_{max}. Zero inhibitor provided the maximum value for $sf(s)$ and gave the plot with the greatest deviation from linearity (Figure 1A). As the concentration of externally added inhibitor was increased, the value of $sf(s)$ declined until the lowest curve in Figure 1A approached the extreme where $\pi af(a) > Nsf(s)$ at all substrate concentrations. The latter closely corresponded to Michaelis−Menten-type kinetics and gave a nearly linear plot.

Alkaline phosphatase provided the unique additional property of product inhibition. In this case, the value of $sf(s)$ varied with externally added inhibitor as well as with the velocity of the enzyme reaction in the periplasm. The theoretical curves shown in Figure 1B were generated by using the assumption that the rate constant for product escape from the periplasm was 4-fold greater than the rate constant for substrate entry ($x = 4.0$, eq 7). The concentration of externally added inhibitor was varied to produce the family of curves shown. The impact of product inhibition was large, as shown by comparison of the uppermost curve (no inhibition) and the second curve from the top (inhibition by product only, Figure 1B). Once again, the addition of a very high concentration of external inhibitor resulted in an approach to diffusional equilibrium, where product inhibition had virtually no impact except by its contribution to the total inhibitor concentration in the medium.

Figure 1C shows a comparison between theoretical curves from Figure 1B and the theoretical expectation for free enzyme at the same inhibitor concentrations. Again, the deviation of the two curves was greatest in the absence of externally added inhibitor. At sufficiently high inhibitor concentrations, the curves were similar, indicating that the reaction was no longer influenced by the diffusion barrier or by the fact that the enzymes were part of a larger particle.

Figure 2A shows the effect of N. The total enzyme concentration in the assay was constant, so that the number of bacteria per assay differed. Equation 4 predicts that, at low [S], where the reaction was limited by substrate diffusion across the outer membrane, the velocity of the reaction will be proportional to cell concentration. Thus, at constant total enzyme, velocity will be higher for reactions containing more cells, despite similar amounts of enzyme per assay. This property has been observed experimentally (Martinez et al., 1992). At high levels of inhibitor (Figure 2A), the results become similar for the two conditions.

A different manner of illustrating the effect of N is at constant cell density. In this case, Figure 2B shows that, at

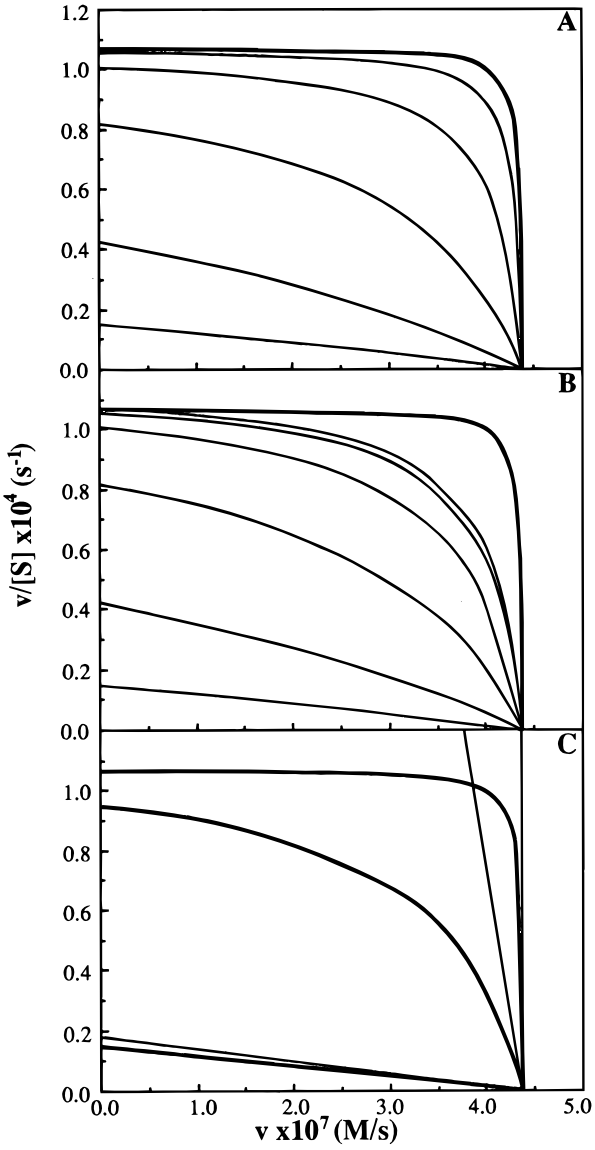

FIGURE 1: Theoretical behavior at constant enzyme levels but varied enzyme efficiency. The constants used to solve eq 6 are given in Materials and Methods. Other values include $f(a) = 4.26 \times 10^{-4}$, $V_{max} = 4.38 \times 10^{-7}$ M/s, [cell] $= 5.33 \times 10^7$/mL, and $N_{tot} = 1.55 \times 10^5$/cell. These values correspond to experimentally observed parameters for alkaline phosphatase. Panel A: Theoretical curves were generated for reactions in the presence of various amounts of an externally added competitive inhibitor ($K_I = 60$ μM). The bold curve shows the results with no inhibitor, and subsequent curves (top to bottom) are for inhibitor concentrations of 2.0×10^{-4}, 1.0×10^{-3}, 5.0×10^{-3}, 2.5×10^{-2}, and 1.0×10^{-1} M. Panel B: Theoretical results corrected for product formed in the periplasm. Product concentration in the periplasm was calculated using a value of 4.0 for x (eq 7, Materials and Methods). The bold line shows the results if no inhibitor was added and no product inhibition occurred. The second curve from the top shows the theoretical results with product inhibition. Subsequent curves show the results for addition of the levels of external inhibitor used in panel A. Panel C: Curves from panel B corresponding to 0, 2, and 100 mM inhibitor (upper to lower curves) are shown in bold. The narrow lines show the behavior for the same amount of free enzyme in the presence of these inhibitor concentrations.

low substrate concentrations, the velocity of the reaction depended on cell concentration and was independent of total enzyme concentration. This property has also been observed (Martinez et al., 1992). Variation of $sf(s)$ by the addition of a competitive inhibitor altered the plot in the manner shown in Figure 1B. Again, at high levels of inhibitor, the behavior

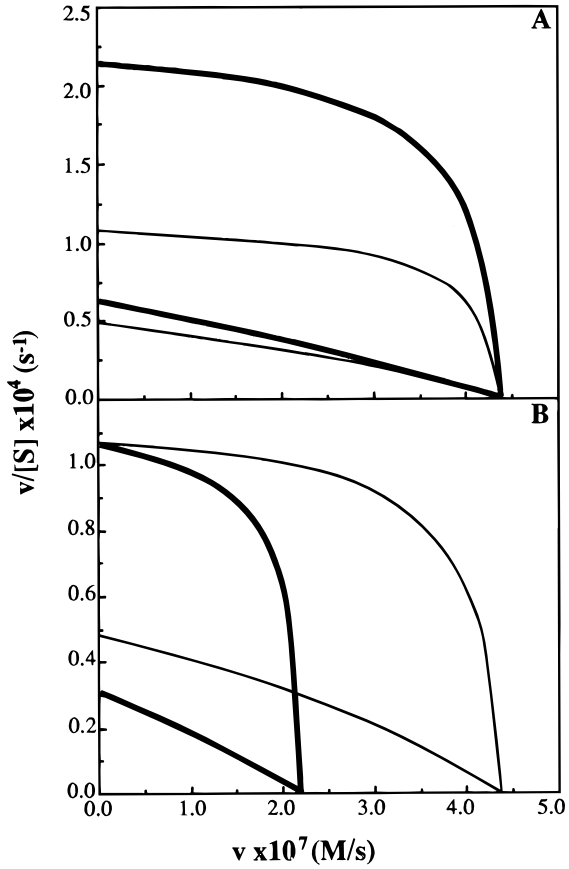

FIGURE 2: Impact of different amounts of enzyme per cell. Theoretical plots are shown for two different cell preparations containing different amounts of enzyme per cell. These are shown at constant enzyme concentration (panel A) or constant cell concentration (panel B). Panel A: The values used to solve eq 6 were the same as in Figure 1A and were corrected for product inhibition ($x = 4$). The bold lines show the results for reactions containing 1.07×10^8 cells/mL and $N_{tot} = 7.75 \times 10^4$/cell. The narrow lines show the results for reactions containing 5.33×10^7 cells/mL and $N_{tot} = 1.55 \times 10^5$/cell. The lower curves show the results when external inhibitor (2.0×10^{-2} M, $K_I = 60$ μM) was added. Panel B: Reactions at constant cell concentration. The values used to solve eq 6 were the same as used in panel A, except that both reactions had the same cell concentration (5.33×10^7/mL) but different numbers of enzymes per cell. Bold lines show the results for $N_{tot} = 7.75 \times 10^4$/cell and $V_{max} = 2.2 \times 10^{-7}$ M/s. The narrow lines show the results for when $N_{tot} = 1.55 \times 10^5$/cell and $V_{max} = 4.38 \times 10^{-7}$ M/s. Again, the two lower curves show the results when inhibitor (2×10^{-2} M) was added to the assay.

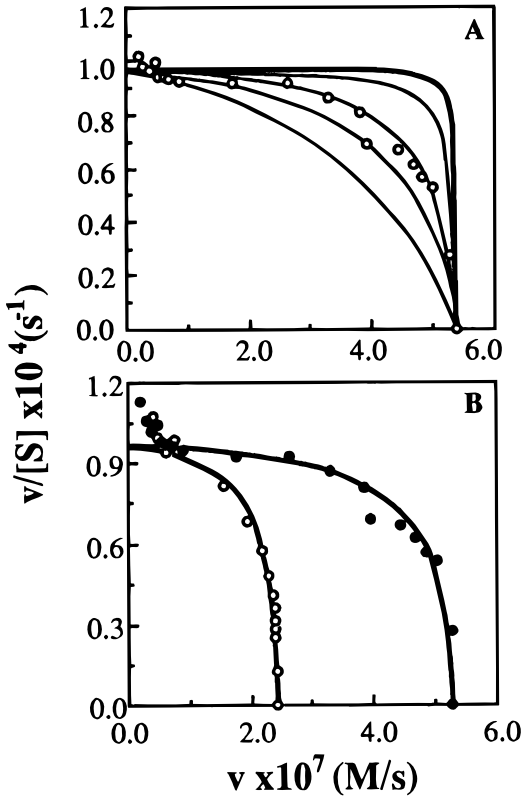

FIGURE 3: Fitting of experimental data. Panel A: Theoretical curves were generated for *E. coli* strain M464E under the following reaction conditions: $V_{max} = 5.4 \times 10^{-7}$ M/s, [cell] $= 5.3 \times 10^7$/mL, $N_{tot} = 1.93 \times 10^5$/cell, and $f(a) = 3.9 \times 10^{-4}$. The latter value was obtained from the average of experimentally determined velocity and substrate concentrations at $v \leq 1.0 \times 10^7$ M/s (the horizontal portion of the graph). The uppermost curve represents the theoretical results for a reaction with no product inhibition. The lowermost curve was corrected for product inhibition and assumed that the rate constant for product escape from the periplasm was identical to that for substrate entry ($x = 1.0$, Materials and Methods). Other curves resulted from x values of 20, 4, and 2 (second, third, and fourth curves from the top, respectively). Panel B: Results for cells with different enzyme density. The M464E strain was induced for different periods of time to obtain different levels of enzyme. Conditions: cell density, 5.27×10^7/mL; V_{max} and N_{tot} were 5.38×10^{-7} M/s and 1.93×10^5/cell (●) and 2.43×10^{-7} M/s and 8.7×10^4/cell (○). Other parameters were the same as in panel A.

of the two situations became similar with plots that were nearly linear and parallel.

Fitting of Experimental Results. Figure 3A shows an Eadie−Hofstee plot of kinetic analysis of alkaline phosphatase in the periplasm of *E. coli* strain M464E. The slight upward curvature of the plots at low velocity was disregarded since it was not always observed (Martinez et al., 1992) and could arise from a small population of cells with damaged or leaky outer membranes.

Outer membrane permeability, $f(a)$, was determined from reaction velocity and substrate concentrations in the horizontal region of the graph, as described in Materials and Methods. The bold line represents the theoretical result when no inhibitors were present. The lower most curve was corrected for product formed in the periplasm, assuming that the rate constant for product escape was identical to that for substrate entry ($x = 1$, eq 7). The other curves were solved in the same manner except that x was assigned values of 20, 4.0, and 2.0 (corresponding to the second, third, and fourth curves from the top, respectively). The best fit to the experimental data was obtained for a value of $x = 4$. This value appeared to be reasonable for the dimensions of these molecules (see the following). This strain of bacteria also gave an excellent fit to experimental data at different numbers of enzymes per cell (Figure 3B).

Optimum fitting of the experimental data could also be achieved by variation of other terms in B (eq 3′), such as K_M or K_I (plots not shown). Together with x, these terms all combine to describe $sf(s)$. Therefore, a 4-fold change in the correct direction provided an optimum fit to the data. Since the product differs from the substrate in size and diffusion properties, it seems probable that a 4-fold difference between product escape and substrate entry may be the only consideration needed to obtain an optimum fit.

Figure 4 shows that this approach allowed the accurate fitting of results for other strains of *E. coli*. Figure 4A shows the result for a wild-type strain that expressed normal levels

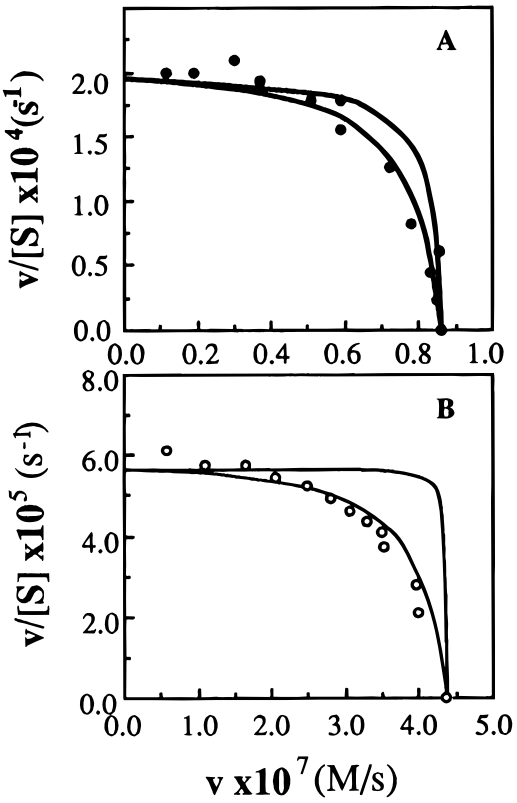

FIGURE 4: Results for other strains of *E. coli*. Panel A: *E. coli* K12 wild-type cells were induced for alkaline phosphatase expression by phosphate starvation. Data are from Martinez et al. (1992). The theoretical curves utilized the parameters given for Figure 3, except for the following: $V_{max} = 8.6 \times 10^{-8}$ M/s, [cell] = 7.47×10^7/mL, $N_{tot} = 2.17 \times 10^4$/cell, and $f(a) = 5.69 \times 10^{-4}$. Again, the upper curve represents the results for a system with no product inhibition. The lower curve is the result for $x = 4.0$ (eq 7). Panel B: Results for *E. coli* strain K12pIV26. The parameters used to solve eq 6 were $V_{max} = 4.4 \times 10^{-7}$ M/s, [cell] = 4.14×10^7/mL, $N_{tot} = 2 \times 10^5$/cell, and $f(a) = 2.9 \times 10^{-4}$.

of alkaline phosphatase and normal porin distributions. Figure 4B shows the result for a similar strain that contained the plasmid and therefore had over-expressed enzyme levels. Both sets of data correlated with theory quite well. This suggested that expression of the enzyme at abnormally high levels did not alter its behavior to a significant degree.

Impact of Externally Added Inhibitor. Figure 5A shows the fit of theory and results for another strain of *E. coli*. This is presented at a varied enzyme level per cell, but constant total enzyme per assay in the manner illustrated in Figure 2A. Addition of *o*-cpp to the assay produced the anticipated result: the differences between the various cell preparations decreased and the plots showed less curvature (Figure 5B). Addition of high levels of *o*-cpp reduced reaction velocity even further and eliminated the difference between the cells. Qualitatively, this is the expected impact of an added inhibitor (Figure 1). Due to the fact that *o*-cpp is hydrolyzed by the enzyme, two inhibitors (both *o*-cpp and inorganic phosphate) are present and theoretical modeling of the data in Figure 5B,C is not possible. Unfortunately, phosphate could not be used as the inhibitor because the concentration required to obtain the needed impact on kinetics also destabilized the bacteria and increased permeability. The results in Figure 5 therefore were limited to the illustration that the general pattern of behavior correlated with theoretical expectations.

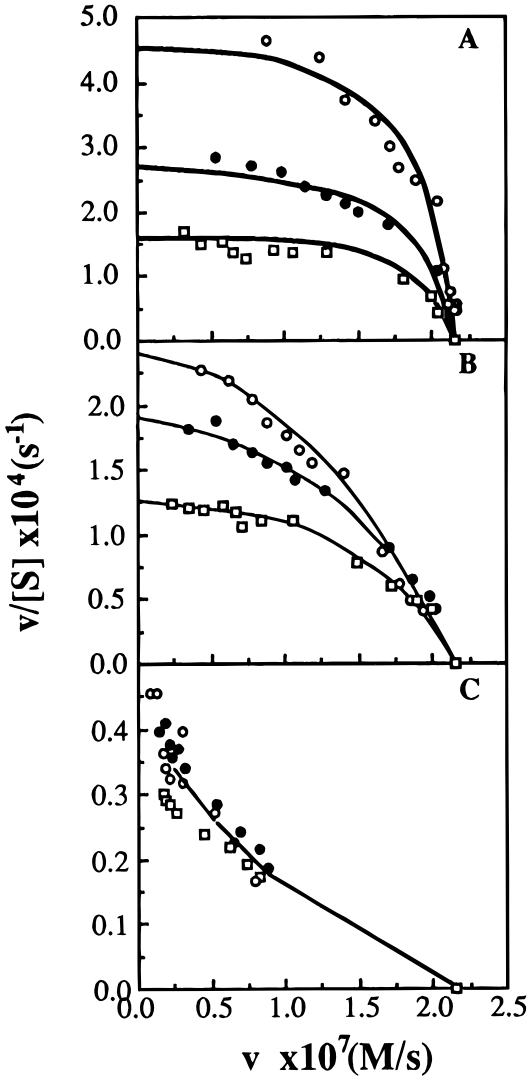

FIGURE 5: Enzyme inhibition by externally added inhibitor. Panel A: Results without externally added inhibitor. Theoretical curves and experimental data are shown for *E. coli* strain MZ9387 pIV26 using the following values: $f(a) = 1.45 \times 10^{-3}$, $V_{max} = 2.15 \times 10^{-7}$ M/s, and $x = 4$. Cell concentrations and N_{tot} for the experiments were as follows: 7.94×10^7/mL, 5.1×10^4/cell (○); 3.06×10^7/mL, 1.3×10^5/cell (●); 2.29×10^7/mL, 1.77×10^5/cell (□). Panel B: Reaction in the presence of intermediate levels of inhibitor. The conditions are the same as in panel A, except that 4.6×10^{-4} M *o*-cpp was included in the assay. Panel C: Reaction kinetics at high inhibitor levels. The conditions are the same as in panel A, except that 4.6×10^{-3}M *o*-cpp was included in the assay. The curves drawn in panels B and C were not derived theoretically.

Temperature Effect on Cell Permeability. The studies shown earlier illustrated that cells grown at different temperatures or that expressed different porins had quite different permeabilities to *p*-npp. This effect could arise from the expression of different numbers and/or different types of porins. The studies shown in Figure 6 were conducted to determine whether cells could produce immediate changes in permeability due to environmental changes, without any alteration in the porins expressed. Cells were grown at 30, 37, and 42 °C to provide variations in porin expression. These were assayed at different temperatures and the value of $f(a)$ was determined. The results suggested a small change (about 2-fold, Figure 6A) in the permeability of the cells when assayed at 25 versus 42 °C. This change was opposite that produced by growth at these different temperatures. That is, growth at high temperature resulted in cells with lower

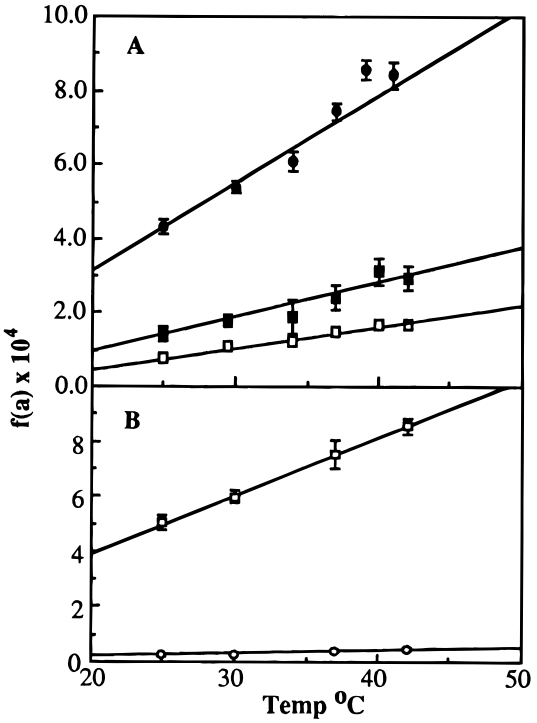

FIGURE 6: Outer membrane permeability as a function of porin expressed and growth and assay temperatures. Panel A: Permeability of cells grown at different temperatures. *E coli* strain K12pIV26 was grown at different temperatures and assayed for alkaline phosphatase activity at the temperatures shown. Cell concentration was varied to give a V_{max} of 4.3×10^{-7} M/s at 37 °C. Cell concentrations for the various cultures were 5.18×10^7/mL for the culture grown at 30 °C (●), 3.63×10^7/mL for the culture grown at 42 °C (□), and 3.83×10^7/mL for the culture grown at 37 °C (■). Cell permeability ($f(a)$) was determined from reaction velocities at low substrate concentrations where velocity was proportional to [S]. The diffusion coefficients used to obtain k_{coll} were adjusted for temperature. Panel B: Permeability of strains expressing only OmpF or OmpC. *E. coli* strains M701FE and M703CE were grown at 37 °C and assayed at the temperatures shown. The value of $f(a)$ was determined as in panel A. Cell concentrations in the assays and V_{max} values were as follows: M701FE, 5.31×10^7/mL, 4.3×10^{-7} M/s (□); M703CE, 4.04×10^7/mL, 4.4×10^{-7} M/s (○). Standard deviations for at least three determinations are shown in both panels.

permeability, while assay at high temperature gave increased permeability. The latter could arise from increased membrane fluidity or other changes that might enhance the channel activity of the porins. In any event, the results suggested that porins were sensitive to temperature, and this might arise from membrane properties. The degree of variation was similar for strains expressing different porins (Figure 6B).

Variation in the ionic strength of the assay solution from 0.5 to 1.5% NaCl had no detectable impact ($<\pm 5\%$) on cell permeability, despite a small enhancement in free enzyme activity by high ionic strength (1.20-fold, data not shown). Overall, it appeared that the regulation of outer membrane permeability was largely achieved by porin expression and that environmental conditions had only a small impact on individual porins once they had been expressed.

DISCUSSION

An earlier study showed how a model for sequestered enzymes could be used to estimate the permeability of the outer membrane of *E. coli* (Martinez et al., 1992). The current study expanded this model to include analysis of the entire range of substrate concentrations as well as to correct for the impact of enzyme inhibitors. The outcome showed excellent correlation between theory and results, indicating that most or all of the reaction parameters had been identified. Given the number of possible impacts that the cell environment could have on the enzyme and substrate, the excellent fit was actually somewhat surprising and has significant implications for enzyme and substrate behavior in the periplasm versus dilute solution.

The theoretical fit required a 4-fold adjustment in enzyme behavior. This could be provided by different rates of product escape versus substrate entry into the periplasm. For example, the phosphate dianion, with a mass of 96 and a density of 1.8, provides an unhydrated sphere with a radius of 0.282 nm. The *p*-npp dianion, with a mass of 218 and a density of 1.6 (the average of 1.8 for the phosphate and 1.48 for *p*-nitrophenol), would produce a sphere with a radius of 0.384 nm. The diffusion constant for product should be 1.36× greater than that of substrate. A smaller cross-sectional area should also allow the product to penetrate the porin channel more readily. Given the solute radii and a channel pore diameter of 1.12 nm (1.08−1.16 nm for OmpF and OmpC; Lakey et al., 1985; Nikaido & Rosenberg, 1983), the relative ability of product versus substrate to enter the channel should be related to the ratio of excess cross-sectional areas provided by the porin for the two solutes [$\pi(0.56 - 0.282)^2/\pi(0.56 - 0.384)^2 = 2.5$]. Hydration to seven waters per ion did not have a large effect on this ratio. Thus, the combined effect of a higher diffusion rate (1.36-fold) and better penetration through the porins (2.5-fold) could provide very near a 4-fold difference in product escape versus substrate entry. This is all that is needed to obtain an optimum fit of theory and results.

Since theoretical modeling for the reaction in the periplasm was based on enzyme behavior in dilute solution, the close correlation of theory and results suggested that enzyme properties in the periplasm were similar to those in dilute solution. This observation may be important for several reasons. A number of studies have used kinetic constants determined *in vitro*, along with enzyme reaction velocity *in vivo* and Fick's law of diffusion, to estimate diffusion through the outer membrane of whole cells (Nikaido et al., 1983; Sen et al., 1988; Todt & Mcgroarty, 1992; Van Alphen et al., 1978). This approach appears to assume that enzyme behavior in the periplasm and in dilute solution is identical. Other approaches to characterize kinetics and permeability also appear to depend on ideal enzyme kinetic behavior in the periplasm (Irwin et al., 1981; Overbeeke & Lugtenberg, 1982). The results of the current study indicated that this assumption was very nearly valid for alkaline phosphatase. This applied to cells with different levels of enzyme and for several strains of *E. coli*.

The excellent fit of theory and results also suggested that the substrate had similar properties in the periplasm and in dilute solution. Similar diffusion properties for small molecules in the cell versus dilute solution were also suggested in recent studies with calcium and cyclic AMP (Bacskai et al., 1993). Thus, for many substances, it appears valid to extrapolate properties of enzymes and substrates from dilute solution to the cellular environment. Naturally, this property will have to be tested for each enzyme and substrate.

Diffusion-limited kinetics may be an evolutionary goal for a number of enzyme systems. This provides that all substrate molecules entering the periplasm are captured by the enzyme. This could be important to trap materials that enter from the external environment or to recycle materials that escape from the cytosol. The number of enzymes per cell that are needed to provide full capture will depend on several factors, including membrane permeability to substrate and enzyme efficiency. Alkaline phosphatase is a highly effective enzyme ($K_M = 15$ μM, $k_{cat} = 32$/s), and only about 20 000 enzymes per cell are produced in wild-type *E. coli* (Figure 4). Another periplasmic enzyme, β-lactamase, has a lower catalytic efficiency ($K_M = 1$ mM, $k_{cat} = 98$/s; Nakaido et al., 1982; M. B. Martinez and G. L. Nelsestuen, unpublished), and a substrate, cephaloridine, appears to be 4−5 times more permeable to the membrane than is *p*-npp. β-Lactamase is expressed at high levels (up to 2×10^6/cell, unpublished). This may illustrate an adaptation that targets efficient substrate capture by both systems. This is achieved by adjusting N to offset differences in K_M, k_{cat}, and membrane permeability. It will be interesting to determine whether other enzymes follow this pattern.

Although results for the addition of large amounts of external inhibitor could not be fit precisely, the general pattern of behavior correlated with expectations. For example, as inhibitor concentration was increased, the behavior of cells containing different levels of enzyme became less divergent and finally indistinguishable. The latter is expected for free enzyme and the Michaelis−Menten condition. Other results indicated that although permeability was altered by temperature, the change was small and probably arose from factors such as the effect of membrane fluidity on porin behavior. The results did not suggest extensive regulation of porins by events such as the time spent in open versus closed conformations.

This study shows that an enzyme reaction, *in vivo*, can be thoroughly modeled if all parameters that influence reaction velocity are known. The overall properties of the *in vivo* reaction deviated greatly from standard Michaelis−Menten behavior. This type of kinetic property may be relatively common for both periplasmic and surface enzymes and receptors [Andree et al., 1994; Billy et al., 1995; reviewed in Abbott and Nelsestuen (1988)]. This behavior can help to achieve a number of goals for an intact organism.

REFERENCES

Abbott, A. J., & Nelsestuen, G. N. (1987) *Biochemistry 26*, 7994.
Abbott, A. J., & Nelsestuen, G. L. (1988) *FASEB J. 2*, 2858.
Adler, J. (1973) *J. Gen. Microbiol. 74*, 77.
Andree, H. A. M., Contino, P. B., Repke, D., Gentry, R., & Nemerson, Y. (1994) *Biochemistry 33*, 4368.
Bacskai, B. J., Hochner, B., Mahaut-Smith, M., Adams, S. R., Kaang, B., Kandel, E. R., & Tsien, R. Y. (1993) *Science 260*, 222.
Berg, H. C., & Purcell, E. M. (1977) *Biophys. J. 20*, 193.
Billy, D., Speijer, H., Willems, G. Hemker, H. C., & Lindhout, T. (1995) *J. Biol. Chem. 270*, 1029.
Georgiou, G., Telford, J. N., Shuler, M. L., & Wilson, D. B. (1986) *Appl. Environ. Microbiol.* 1157.
Goldstein, L. (1976) *Methods Enzymol. 44*, 397.
Goldstein, B. (1989) *Comments Theor. Biol. 1*, 109.
Goldstein, B., & Wiegel, F. W. (1983) *Biophys. J. 43*, 121.
Irwin, R. T., MacAlister, T. J., & Costerton, J. W. (1981) *J. Bacteriol. 145*, 1397.
Laidler, K. J., & Bunting, P. S. (1980) *Methods Enzymol. 64*, 397.
Lakey, J. H., Watts, J. P., & Lea, E. J. A. (1985) *Biochim. Biophys. Acta 817*, 208.
Laurent, T. (1963a) *Biochem. J. 89*, 253.
Laurent, T. C. (1963b) *Biochem. J. 89*, 249.
Laurent, T. C. (1971) *Eur. J. Biochem. 21*, 498.
Martinez, M. B., Schendel, F. J., Flickinger, M. C., & Nelsestuen, G. L. (1992) *Biochemistry 31*, 11500.
Minton, A. P. (1983) *Mol. Cell. Biochem. 55*, 119.
Nikaido, H., & Rosenberg, E. Y. (1983) *J. Bacteriol. 153*, 241.
Nikaido, H., Rosenberg, E. Y., & Foulds, J. (1982) *J. Bacteriol. 153*, 232.
Overbeeke, N., & Lugtenberg, B. (1982) *Eur. J. Biochem. 126*, 113.
Schendel, F. J., Baude, E. J., & Flickinger, M. C. (1989) *Biotechnol. Bioeng. 34*, 1023.
Sen, K., Hellman, J., & Nikaido, H. (1988) *J. Biol. Chem. 263*, 1182.
Sundaram, P. V., Tweedale, A., & Laidler, K. J. (1970) *Can. J. Chem. 48*, 1498.
Sutcliffe, J. G. (1978) *Proc. Natl. Acad. Sci. U.S.A. 75*, 3737.
ter Kuile, B. H., & Cook, M. (1994) *Biochim. Biophys. Acta 1193*, 235.
Todt, J. C., & Mcgroarty, E. J. (1992) *Biochem. Biophys. Res. Commun. 189*, 1498.
Van Alphen, W., Van Boxtel, R., Van Selm, N., & Lugtenberg, B. (1978) *FEMS Microbiol. Lett. 3*, 103.
Wiley, H. S. (1988) *J. Cell Biol. 107*, 801.
Zimmerman, S. B. (1993) *Annu. Rev. Biophys. Biomol. Struct. 22*, 27.

BI951955A